



Interactions between the WEE-1.3 kinase and the PAM-1 aminopeptidase in oocyte maturation and the early *C. elegans* embryo

Dorothy Benton,^{1,†} Eva C. Jaeger,¹ Arielle Kilner,^{1,2} Ashley Kimble,¹ Josh Lowry,³ Emily M. Schleicher,^{1,‡} Kaiden M. Power ,^{1,§} Danielle Uibel,¹ Caprice Eisele,¹ Bruce Bowerman ,³ and Rebecca Lyczak^{1,*}

¹Biology Department, Ursinus College, 601 E Main Street, Collegeville, PA 19426, USA

²Biomedical Studies Department, Graduate School of Biomedical Sciences and Professional Studies, Drexel University College of Medicine, 2900 W. Queen Lane Philadelphia, PA 19129, USA

³Institute of Molecular Biology, 1229 University of Oregon, 1318 Franklin Blvd., Eugene, OR 97403, USA

[†]Present address: Drexel University College of Medicine, Philadelphia, PA 19102, USA.

[‡]Present address: Department of Biochemistry and Molecular Biology, The Pennsylvania State University College of Medicine, Hershey, PA 17033, USA.

[§]Present address: Genetics Department, Rutgers, the State University of New Jersey, Piscataway, NJ 08854, USA.

*Corresponding author: Ursinus College Biology Department, 601 E Main Street, Collegeville, PA 19426, USA. rlyczak@ursinus.edu

Abstract

Puromycin-sensitive aminopeptidases are found across phyla and are known to regulate the cell-cycle and play a protective role in neurodegenerative disease. PAM-1 is a puromycin-sensitive aminopeptidase important for meiotic exit and polarity establishment in the one-cell *Caenorhabditis elegans* embryo. Despite conservation of this aminopeptidase, little is known about its targets during development. In order to identify novel interactors, we conducted a suppressor screen and isolated four suppressing mutations in three genes that partially rescued the maternal-effect lethality of *pam-1* mutants. Suppressed strains show improved embryonic viability and polarization of the anterior–posterior axis. We identified a missense mutation in *wee-1.3* in one of these suppressed strains. WEE-1.3 is an inhibitory kinase that regulates maturation promoting factor. Although the missense mutation suppressed polarity phenotypes in *pam-1*, it does so without restoring centrosome–cortical contact or altering the cortical actomyosin cytoskeleton. To see if PAM-1 and WEE-1.3 interact in other processes, we examined oocyte maturation. Although depletion of *wee-1.3* causes sterility due to precocious oocyte maturation, this effect was lessened in *pam-1* worms, suggesting that PAM-1 and WEE-1.3 interact in this process. Levels of WEE-1.3 were comparable between wild-type and *pam-1* strains, suggesting that WEE-1.3 is not a direct target of the aminopeptidase. Thus, we have established an interaction between PAM-1 and WEE-1.3 in multiple developmental processes and have identified suppressors that are likely to further our understanding of the role of puromycin-sensitive aminopeptidases during development.

Keywords: polarity; oocyte maturation; puromycin-sensitive aminopeptidase; suppressors; Myt1 kinase; *C. elegans*

Introduction

The M1 family of zinc metalloproteases is a highly conserved aminopeptidase group that regulates peptide processing, protein degradation, and the cell cycle. Members are characterized by a HEXXH[18X]E, Zinc coordination site and the GXMXN catalytic domain. Family members can be cytoplasmic or membrane associated and have been shown to cleave either a single or series of N-terminal amino acids, often from small peptides (reviewed in Peer 2011).

Within this family are the puromycin-sensitive aminopeptidases (PSAs) that are involved in cell-cycle regulation in many species. PAM-1 is a highly conserved PSA in *Caenorhabditis elegans* with homologs regulating fertility and meiosis in numerous organisms (Osada et al. 2001; Brooks et al. 2003; Sánchez-Morán et al. 2004). In *C. elegans*, PAM-1 and other metalloproteases in the family interact in the gonad to ensure fertility and fecundity

(Althoff et al. 2014). Both mammalian cells and *Dictyostelium* require functional PSA for proper progression through the cell cycle (Constam et al. 1995; Poloz et al. 2012). In *Dictyostelium*, PSA is known to associate with Cdk5, and loss of Cdk5 shows similar phenotypes to inhibition of PSA (Sharma et al. 2002; Huber and O'Day 2011; Huber et al. 2013). Despite this interaction, the mechanism by which these aminopeptidases control fertility and cell-cycle progression is unknown. In addition to cell-cycle control, recent work with a human homolog, NPEPPS, suggest that the protein may play a neuroprotective role by degrading Tau and SOD1 (Yanagi et al. 2009; Kudo et al. 2011; Ren et al. 2011). Due to the many phenotypes associated with loss of these aminopeptidases, it is likely there are unexplored targets.

Caenorhabditis elegans provides a unique system for studying this aminopeptidase family and identifying interacting proteins (Brooks et al. 2003; Lyczak et al. 2006). The cytoplasmic

Received: December 29, 2020. Accepted: February 23, 2021

© The Author(s) 2021. Published by Oxford University Press on behalf of Genetics Society of America.

This is an Open Access article distributed under the terms of the Creative Commons Attribution-NonCommercial-NoDerivs licence (<http://creativecommons.org/licenses/by-nc-nd/4.0/>), which permits non-commercial reproduction and distribution of the work, in any medium, provided the original work is not altered or transformed in any way, and that the work is properly cited. For commercial re-use, please contact journals.permissions@oup.com

aminopeptidase, PAM-1 is highly expressed in the early embryo and regulates timely exit from meiosis (Lyczak et al. 2006; Fortin et al. 2010). In the absence of PAM-1, defects in chromosome segregation are observed, and the timing of meiotic exit is significantly extended. In addition, PAM-1 regulates centrosome positioning at the posterior cortex of the embryo to ensure establishment of the anterior–posterior axis (Fortin et al. 2010; Saturno et al. 2017).

In wild-type, the centrosome cues polarization of the one-cell embryo, resulting in cortical flows, pseudocleavage, localization of PAR proteins to anterior and posterior domains, and an asymmetric cell division (reviewed in Rose and Gönczy 2014). In *pam-1* mutants, reduced centrosome–cortical contact prevents polarity establishment resulting in reduced cortical flows and pseudocleavage. This leads to mislocalization of the cortical PAR proteins and a symmetric first cleavage and embryonic lethality (Lyczak et al. 2006; Fortin et al. 2010; Saturno et al. 2017). When centrosome contact is maintained with the posterior cortex, these polarity defects are rescued, leading to the model that PAM-1 regulates polarity through the centrosome (Fortin et al. 2010). However, nothing is known about the targets and protein interactors PAM-1 may work with to regulate these developmental processes.

To learn more about the targets and protein interactors of PAM-1, we implemented a suppressor screen as an unbiased approach to identify genetic interactors (reviewed in Hodgkin 2005). Here, we describe the isolation and initial characterization of suppressors of *pam-1* (*spam* mutants), that increase the embryonic viability and partially rescue polarity defects in the early embryo. We have identified a mutation in the gene *wee-1.3* in one of these suppressors. In order to understand how the cell-cycle regulator WEE-1.3 and the aminopeptidase PAM-1 interact, we looked at suppression phenotypes and for genetic interactions in polarity establishment and oocyte maturation. Here we report evidence that PAM-1 and WEE-1.3 work together in both of these processes.

Materials and methods

Strains and maintenance

Strains were propagated on NGM plates at 15°C as described (Brenner 1974). The N2 Bristol strain was used as wild-type and the CB4856 strain was used for mapping. The alleles used in this study were: *pam-1(or347)*, *pam-1(or403)*, *spam-2/wee-1.3(lz5)*, *wee-1.3(syb1738)*, *wee-1.3(q89eb60)*, *wee-1.3(ana8 [wee-1.3::gfp])* (Fernando et al. 2021), *unc-24(e138)*, *spam-1(lz3)*, *spam-1(lz4)*, *spam-3(lz6)*, *nmy-2(cp13[nmy-2::gfp + LoxP])*. The following transgenes were used in this study: *ddl56[tbg-1::GFP + unc119 (+)]*, *axls1327[par-1::GFP]*.

Creation of CRISPR strain

To recreate the mutation identified in *wee-1.3(lz5)*, SunyBiotech Corporation was contracted to produce a CRISPR mutation that would result in the identical amino acid change in WEE-1.3. The strain constructed by SunyBiotech was designed to have the *lz5* missense as well as three silent mutations necessary to perform the CRISPR edit and prevent recutting (Supplementary Figure S1). The following guide RNAs were used: Sg1: CCACCAAACGCGC AACGCCGTTT and Sg2: CCGGAGAGTCCGCCGAGAATGAA. The edits were made with a donor plasmid containing the missense mutation as well as changes to prevent recutting of the sequence were included (Supplementary Figure S1). The sequence of the new strain (PHX1738: *wee-1.3(syb1738)*) was confirmed by

SunyBiotech Corporation as well as independently by Sanger sequencing once the strain was received using primers RL01-seq-s: TGCTTGACTCTGATCCGAGG and RL01-seq-a: TCTTCTACGT GGCGATTCCG or WEE-1F: TCTGATCCGAGGATTCGTCC and WEE-1R: GGCATTCTCGGTAGATCAG.

RNAi

Worms were fed RNA interference (RNAi) bacteria as described (Kamath and Ahringer 2003). Worms were placed at 25°C for 20 hours prior to imaging or for other times indicated in time-course experiments. Phenotypes of *wee-1.3(RNAi)* worms were compared with those treated with an empty RNAi vector (L4440).

For time-course experiments, worms were placed on RNAi bacteria for 24 hours at 25°C. Worms were then transferred to individual RNAi plates every 2 hours and the number of embryos laid was recorded at each transfer.

Suppressor screen

We conducted a suppressor screen to identify proteins that may interact with PAM-1 in the early embryo. Worms with a missense mutation in *pam-1(or347)*, were mutagenized with EMS as previously described (Encalada et al. 2000). Mutagenized F2 worms were grown at a nonpermissive temperature of 25°C where nearly all embryos laid fail to hatch. Worms surviving on plates after 2 weeks were single picked and tested for embryonic viability. Worms with progeny that showed a consistently elevated viability were outcrossed for further analysis.

Embryonic viability

L4 worms were single picked onto plates at 20°C overnight. The next day the adult was removed and the embryos laid were counted. The following day, hatching progeny were counted and embryonic viability calculated (number of hatched progeny/total embryos laid).

Brood analysis

L4 worms were single plated to 20°C and transferred to fresh plates every 24 hours for 72 hours. After worms were removed from each plate, the number of embryos laid was counted and the total from 72 hours of laying were totaled. Data from 20 worms were averaged and standard deviation determined.

SNP mapping

unc-24(e138), *pam-1(or347)*; *spam* worms were mated to the polymorphic Hawaiian strain CB4856. F2 worms were screened by testing for the presence of *pam-1* by screening for N2 SNPs flanking the locus as well as the presence of the closely linked *unc-24* marker. These worms were then tested for embryonic viability at levels comparable to the suppressed strain. Each rehomozygous strain became a mapping line for SNP mapping. SNP mapping of lines was performed as described (Davis et al. 2005).

Sequencing

Whole-Genome Sequencing

Six mapping lines for the *spam* allele *lz5* were created using the above methods. DNA was isolated from these lines for whole-genome sequencing (WGS) as described (O'Rourke et al. 2011; Lowry et al. 2015). Data analysis was performed using a local Galaxy installation running the CloudMap pipeline (modified from Minevich et al. 2012). Mapping regions were identified by the absence of CB4856 SNPs as determined by plotting allele frequency versus chromosomal position. Thirteen variants (10 that changed coding regions) were identified in the area. Each was

tested individually for suppressing ability. Based on the combination of our SNP mapping data and WGS data, the location of the lz5 mutation was determined to be located in the gene *wee-1.3*. Sanger sequencing was then performed on the *wee-1.3(lz5)* allele (forward primer: TCTGATCCGAGGATTCGTCC; reverse primer: GGCATTCTCGGTAGATCAG) to further confirm the mutation.

Microscopy

For gonad imaging, worms were anesthetized in 0.1% tricaine/tetramisole as described (McCarter et al. 1999) and imaged on a 3% agarose pad or were immobilized on a 6% agarose pad with 2 μ l of a 50% solution of 0.1 μ m diameter polystyrene microspheres (Kim et al. 2013). For embryo imaging, embryos were released on a coverslip and imaged on a 3% agarose pad.

For DIC and time-lapse imaging, a Nikon DS-Fi3 microscope camera using NIS Elements imaging software version 4.60 was used and acquisition was performed as described (Lyczak et al. 2006). For confocal and time-lapse imaging, a EZ-C3 Nikon Confocal microscope and NIS Elements software was used. PAR-1, centrosome, and NMY-2 fluorescence imaging was performed as previously described (Saturno et al. 2017).

Scoring and analysis

Gonads examined with DIC microscopy were scored for the presence of nucleoli, checking through multiple focal planes. The oocytes were numbered using distance from the spermatheca, with the closest oocyte at the -1 position and the furthest oocyte counted being the -5 position.

For scoring early embryo polarity, DIC and confocal analysis were used. DIC polarity landmarks, pseudocleavage, and asymmetric cell division were scored for each time-lapse. Centrosome distance from the cortex and PAR-1 domains were measured as described (Saturno et al. 2017). Size and number of NMY-2 foci were determined using NIS-Elements EZ-C2 confocal software. Maximum projections were created from a Z-stack of five images (0.5 μ m apart) of the cortex on one side of the embryo (closest to the coverslip). Foci $>0.5\mu\text{m}^2$ were counted at -700 and -500 seconds prior to nuclear envelope breakdown (NEBD) and their area was determined with ROI statistics.

For WEE-1.3 levels, confocal images were taken of *wee-1.3* (*ana8 [wee-1.3::gfp]*), and *pam-1(or403)*; *wee-1.3* (*ana8 [wee-1.3::gfp]*) with identical settings. A Z-stack of 5 images 0.5 μ m apart were taken for analysis. To calculate WEE-1.3 levels, Z-stacks were turned into maximum intensity projections. The cytoplasm of each oocyte was traced and ROI statistics in the confocal software was used to determine the mean pixel intensity of GFP in each oocyte.

Statistical analysis

Chi Square analysis was used to test for significant differences in embryonic viability, oocyte maturation, and polarity landmarks. In order to determine differences in WEE-1.3 GFP intensity, a weighted one-way ANOVA was performed. For NMY-2 foci size and sterility, a two-tailed, homoscedastic Student's T Test was used. P-values were considered significant at the 0.05 alpha level.

Results

Suppressors of *pam-1* improve the embryonic viability and rescue polarity phenotypes

In a screen for suppression of the maternal-effect embryonic lethality of *pam-1*, we identified four suppressing alleles. Each suppressor was confirmed to act recessively and improved the embryonic viability of a missense allele of *pam-1(or347)* to varying

extents (Table 1). *pam-1(or347)* has a missense allele in the active site required for aminopeptidase activity. Phenotypically it is identical to our null alleles of *pam-1* (Lyczak et al. 2006). Each suppressor was mapped to a broad chromosomal region using SNP mapping (Davis et al. 2005) away from *pam-1*'s position on LG IV. lz3, lz4, and lz6 all mapped to LG I, whereas lz5 mapped to LG II. Complementation testing was performed on suppressors that mapped to LG I. Trans-heterozygotes of lz6 with lz3 or lz4 produced less suppression than for either suppressor mutation alone, indicating that they are unique suppressors. However, the lz3 and lz4 alleles were determined to be mutations in the same gene, as evidenced by a high rescue of embryonic viability in the F1 generation (Table 2). Thus, we named the suppressors, *spam-1(lz3)*, *spam-1(lz4)*, *spam-2(lz5)*, and *spam-3(lz6)*.

Since *pam-1* embryos lack early signs of polarization, we used DIC microscopy to test if these polarity defects were rescued by each suppressor. Each suppressed strain was imaged during the first cell division and signs of polarization were scored. In wild-type, pseudocleavage prior to the first asymmetric cell division is a sign of cortical polarization in the embryo. In *pam-1(or347)* mutants, fewer embryos undergo pseudocleavage and divide asymmetrically due to defects in polarity establishment (Lyczak et al. 2006). However, each suppressor mutation increased the prevalence of both pseudocleavage and an asymmetric division, suggesting a partial rescue of polarity establishment in suppressed embryos (Figure 1). For instance, *pam-1(or347)*; *spam-2(lz5)* embryos increased the presence of pseudocleavage from 28% to 61% and the asymmetric cell division from 55% to 79% as compared with *pam-1(or347)* embryos alone. Similar rescue was observed for other suppressor mutations as well (Figure 1).

wee-1.3(lz5) is a suppressor of *pam-1*

We conducted further work on one of our suppressors, *spam-2(lz5)*. We crossed *spam-2(lz5)* into a nonsense and missense allele of *pam-1* to determine if the suppression of *pam-1* was allele specific. *spam-2* improved embryonic viability of both *pam-1* alleles, but to different extents (Tables 1 and 3). Suppression of the nonsense allele (*or403*) was also observed, increasing viability from 12% to 44%. In comparison, the missense allele (*or347*) showed an increased viability from 7% to 20% (Tables 1 and 3). The difference in suppression between the two *pam-1* alleles was significant ($P < 0.001$). Using SNP mapping, we localized *spam-2(lz5)* to LG II. This was subsequently confirmed by WGS (Figure 2A). In this region, a G to A point mutation at position 1459 in *wee-1.3* was discovered, which resulted in a E487K missense mutation (Figure 2B and Figure S1). This region of the protein is not highly conserved among different species (Lamitina and L'Hernault 2002) and has no domains known to be important for protein

Table 1 Suppressors act recessively to rescue the embryonic lethality of *pam-1* worms

Genotype	Embryonic viability
<i>pam-1(or347)</i>	7.1%
<i>pam-1(or347)</i> ; lz3	51.42%
<i>pam-1(or347)</i> ; lz3/+	0.57%
<i>pam-1(or347)</i> ; lz4	72.06%
<i>pam-1(or347)</i> ; lz4/+	5.52%
<i>pam-1(or347)</i> ; lz5	20.09%
<i>pam-1(or347)</i> ; lz5/+	7.96%
<i>pam-1(or347)</i> ; lz6	78.53%
<i>pam-1(or347)</i> ; lz6/+	8.5%

Embryonic viability was determined at 20°C.

Table 2 Complementation tests of suppressors mapping to LG I: three alleles of two suppressor loci

Genotype	Embryonic viability
<i>pam-1(or347); lz3/lz4</i>	58.59%
<i>pam-1(or347); lz3/+ lz6/+</i>	20.38%
<i>pam-1(or347); lz4/+ lz6/+</i>	37.30%

Embryonic viability of F1 progeny at 20°C. Although all alleles showed an interaction, only *lz3/lz4* fully failed to complement.

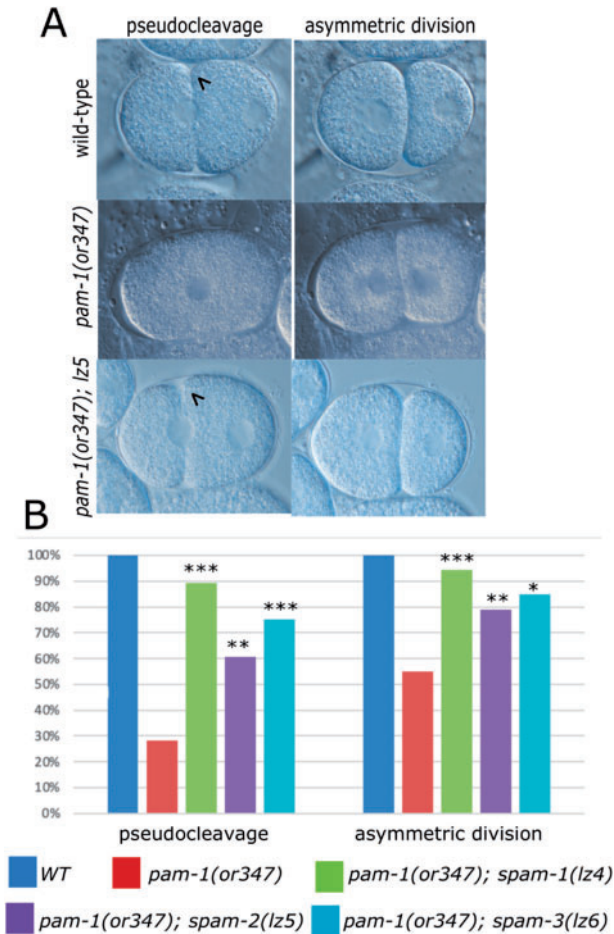


Figure 1 *spam* mutations restore polarity to *pam-1* embryos (A) DIC images show that wild-type embryos exhibit pseudocleavage (arrowhead; $n = 19$) during axis polarization and divide asymmetrically ($n = 44$). Many *pam-1(or347)* embryos do not exhibit pseudocleavage ($n = 39$) or an asymmetric division ($n = 79$), but the presence of a suppressor mutation improves both pseudocleavage (arrowhead) (*lz4* $n = 28$; *lz5* $n = 46$; *lz6* $n = 20$) and the asymmetric division (*lz4* $n = 54$; *lz5* $n = 85$; *lz6* $n = 20$) in many embryos. Anterior to the left. (B) Quantification of DIC time-lapse data. Chi square analysis was used to compare *pam-1* embryos to each suppressed strain. * $P < 0.05$; ** $P < 0.01$; *** $P < 0.001$

function. The amino acid change is more C terminal to the ATP binding, kinase, and transmembrane domains. Despite this, a link between a cell-cycle regulator and PAM-1 could provide important insights into its function. We refer to *spam-2(lz5)* as *wee-1.3(lz5)* below.

To determine if the mutation in *wee-1.3* affected its function, we crossed the *wee-1.3(lz5)* mutation away from *pam-1* to see if the worms had any phenotypes associated with *wee-1.3* loss or gain-of-function. Loss of WEE-1.3 function is known to affect oocyte maturation and embryonic survival, whereas

Table 3 Mutations in *wee-1.3* suppress *pam-1* lethality but have no effect on their own

Genotype	Embryonic viability at 20°C
+/+	94.94%
<i>pam-1(or403)</i>	12.4%
<i>pam-1(or403); wee-1.3(lz5)</i>	43.9%***
<i>pam-1(or403); wee-1.3(syb1738)</i>	43.0%***
<i>wee-1.3(lz5)</i>	93.13%
<i>wee-1.3(q89eb60)</i>	5.33%
<i>wee-1.3(q89eb60)/wee-1.3(lz5)</i>	67.49%
<i>wee-1.3(syb1738)</i>	95.0%

Chi square analysis was used to compare the embryonic viability of *pam-1(or403)* with the *wee-1.3* mutations.

*** $P < 0.001$.

gain-of-function mutations affect spermatogenesis and male fertility (Lamitina and L'Hernault 2002; Burrows et al. 2006). Embryos produced by *wee-1.3(lz5)* worms had viability similar to wild-type and oocyte maturation appeared unaffected (Table 3 and see below). In addition, the brood size of *wee-1.3(lz5)* worms (287 ± 52) was comparable to wild-type (281 ± 62). We then created a compound heterozygote with *wee-1.3(lz5)* and *wee-1.3(q89eb60)*, an allele known to be recessive maternal-effect lethal (Lamitina and L'Hernault 2002). This strain showed an intermediate level of lethality, but worms heterozygous for *wee-1.3(q89eb60)* show no lethality on their own. This suggests that *wee-1.3(lz5)* may partially disrupt its function (Table 3).

In order to confirm that the change in *wee-1.3* was in fact the suppressing mutation, we created a CRISPR strain with an identical missense mutation G1459A(E487K), *wee-1.3(syb1738)* (Figure 2B and Figure S1). Similar to *wee-1.3(lz5)*, *wee-1.3(syb1738)* exhibited no differences from wild-type in embryonic viability, oocyte maturation, or brood size (298 ± 62) (Table 3 and see below). In addition, males were fertile and used for numerous matings. When crossed into *pam-1(or403)*, *wee-1.3(syb1738)* suppressed the embryonic lethality of *pam-1* (Table 3), thus confirming *wee-1.3(lz5)* as the suppressing mutation.

wee-1.3(lz5) suppresses the polarity defects of *pam-1*

Since *wee-1.3(lz5)* rescued viability of embryos laid by *pam-1* worms, we decided to look in more detail at polarity establishment in the suppressed strains. Similar to what we observed for suppression of *pam-1(or347)*, polarity was rescued in many *pam-1(or403); wee-1.3(lz5)* mutants. Although only 45.6% of *pam-1(or403)* embryos divided asymmetrically, 79.6% of *pam-1(or403); wee-1.3(lz5)* embryos did (Figure 3A). In wild-type, the PAR proteins localize to anterior or posterior cortical domains during polarization (reviewed in Nance and Zallen 2011). To look at this, we then examined the localization and size of the posterior PAR-1 domain. Previously, we found that a little over half of *pam-1* embryos had posterior localization of PAR-1 and that this domain was on average smaller than wild-type (31% as compared with 42% embryo length; Saturno et al. 2017). In the presence of the *wee-1.3(lz5)* suppressor, we found that 100% of the embryos now showed posterior PAR-1 localization and that PAR-1 was restored to a wild-type domain size of 43% embryo length (Figure 3B and Table 4). Thus, the increase in embryonic viability was accompanied by a restoration of polarity establishment in many embryos.

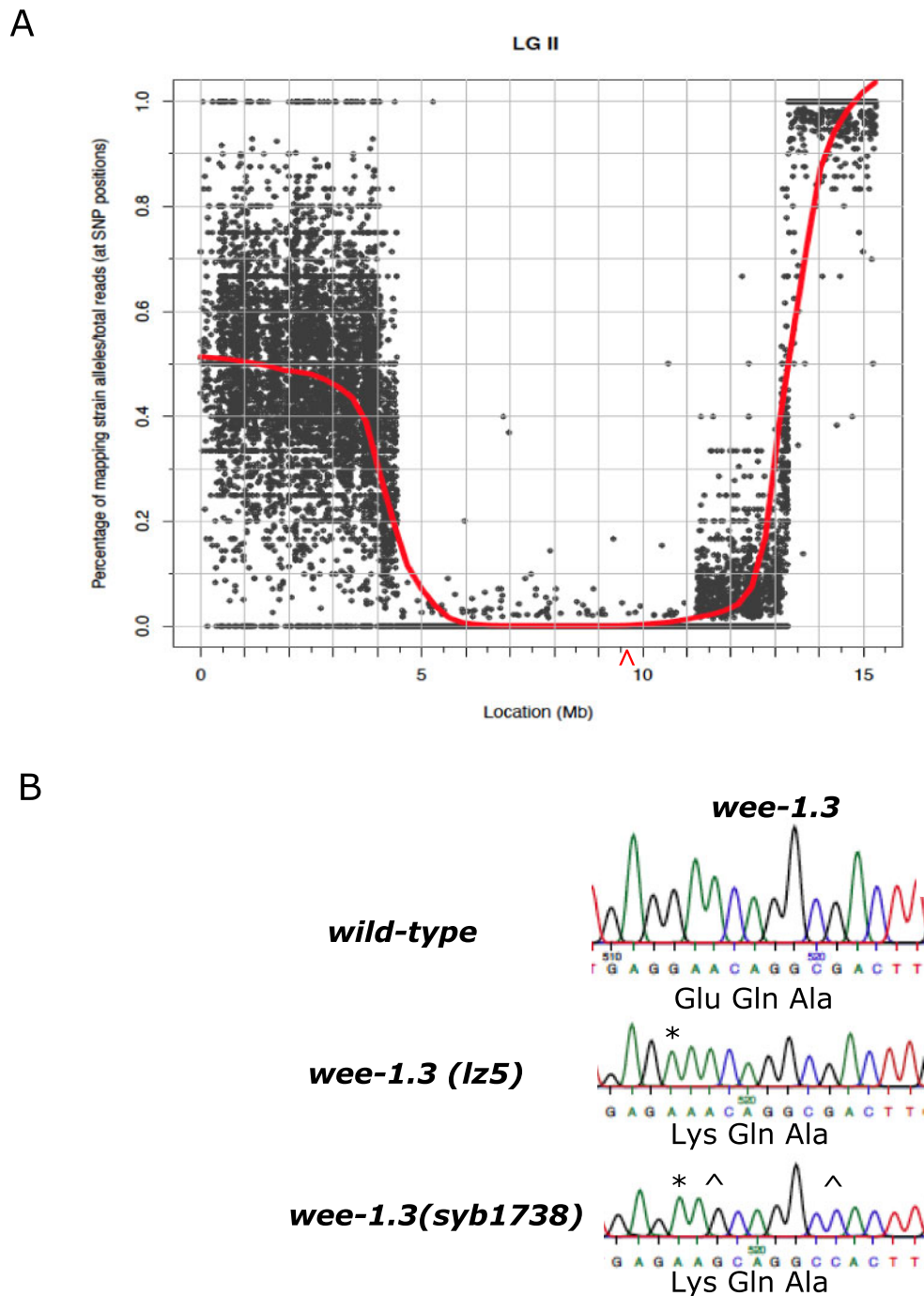


Figure 2 *spam-1(lz5)* maps to LG II and has a missense mutation in *wee-1.3*. (A) Plotting the allele frequency of known Hawaiian SNPs against chromosomal position reveals an ~6.5 Mb region on LG II that contains *spam-2(lz5)*. Allele frequencies were obtained by WGS of mapping lines generated by crossing *pam-1(or347); spam-2(lz5)* worms to Hawaiian males. A missense variant was detected in the gene *wee-1.3*. Red line = LOESS regression trendline. The approximate position of *wee-1.3* is marked by a red arrowhead. (B) Sanger sequencing was used to confirm the presence of the *wee-1.3* missense mutation in our strains. The *wee-1.3(lz5)* allele has a G1459A(E487K) mutation (*). The CRISPR recreated *wee-1.3(syb1738)* strain had the identical change (*), as well as some silent mutations (^) that were introduced to prevent recutting by Cas9; A1461G and G1467C are shown here. All sequences are from strains in the *pam-1(or403)* background.

***wee-1.3(lz5)* suppression of *pam-1* polarity defects is not mediated by changes to the centrosome or actomyosin network**

Our previous work demonstrated that the centrosome is mislocalized in *pam-1* embryos and spends less time in close proximity to the posterior cortex, resulting in poor polarity

establishment (Saturno et al. 2017). Thus, we measured centrosome–cortex contact in *pam-1(or403); wee-1.3(lz5)* worms to see if polarity rescue occurred by extending the time of this contact. In *pam-1(or403)* embryos, the centrosome fails to touch the posterior in 14% of embryos (Saturno et al. 2017). In *pam-1(or403); wee-1.3(lz5)* embryos, 27% did not have

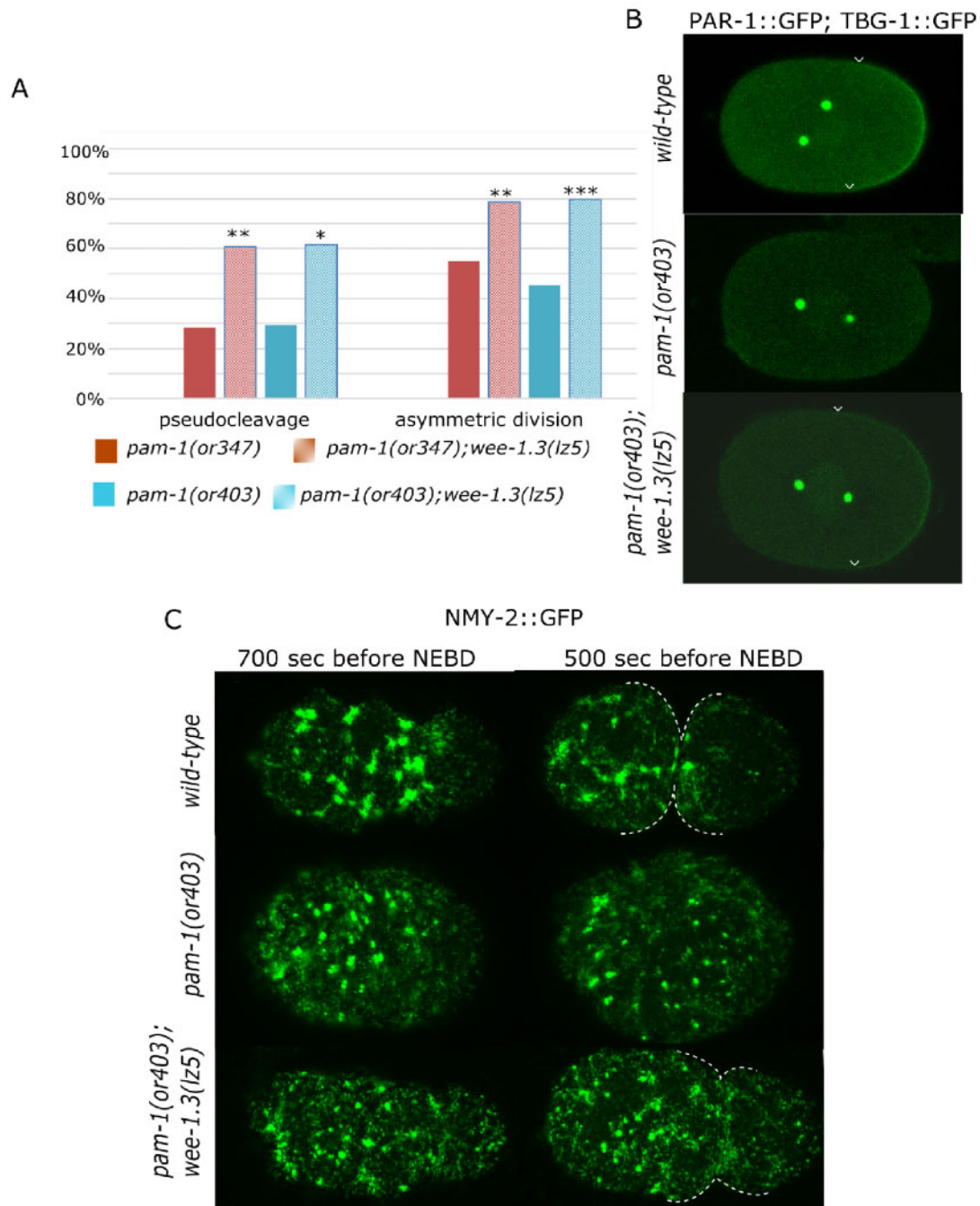


Figure 3 Polarity is improved in *pam-1; wee-1.3(lz5)* embryos. (A) *wee-1.3(lz5)* suppresses polarity defects of two *pam-1* alleles. The presence of pseudocleavage in *pam-1(or347)* ($n = 39$) and *pam-1(or403)* ($n = 27$) is increased in *pam-1(or347); wee-1.3(lz5)* ($n = 46$) and *pam-1(or403); wee-1.3(lz5)* ($n = 34$). Similarly, while many *pam-1(or347)* ($n = 78$) and *pam-1(or403)* ($n = 46$) embryos divide symmetrically, the presence of an asymmetric first cleavage is improved in *pam-1(or347); wee-1.3(lz5)* ($n = 85$) and *pam-1(or403); wee-1.3(lz5)* ($n = 54$) embryos. (B) PAR-1 and gamma-tubulin GFP confocal images. PAR-1 localizes to the posterior in wild-type during polarization. Arrowheads mark the edges of the PAR-1 domain. Although many *pam-1(or403)* embryos lack posterior PAR-1 localization (Saturno et al. 2017), 100% of *pam-1(or403); wee-1.3(lz5)* embryos have posterior localization of PAR-1 in a domain size similar to wild-type ($n = 46$). (C) NMY-2::GFP images show clearing from the posterior in wild-type, 700 seconds prior to NEBD and full pseudocleavage 200 seconds later ($n = 18$). Both *pam-1(or403)* ($n = 18$) and *pam-1(or403); wee-1.3(lz5)* ($n = 13$) embryos often lack posterior clearing. Shown here is reduced clearing in both strains, but pseudocleavage is restored in the presence of the suppressor. Pseudocleavage is marked by dotted lines. Anterior to the left in all panels. * $P < 0.05$; ** $P < 0.01$; *** $P < 0.001$

centrosome–cortical contact ($n = 26$). Of the embryos that exhibited contact, contact time was comparable to *pam-1* alone, being 2.02 minutes in *pam-1; wee-1.3(lz5)* embryos and 2.14 minutes in *pam-1* embryos (Saturno et al. 2017). Both suppressed and non-suppressed strains showed shorter centrosome contact times than seen in wild-type (3.25 minutes;

Saturno et al. 2017). Thus, the rescue of polarity in *pam-1; wee-1.3(lz5)* embryos is not a result of sustained centrosome contact with the cortex.

Next, we looked at the cortical network of nonmuscle myosin, NMY-2, that mediates cortical polarization in response to the centrosomal cue. During polarization, NMY-2 foci in the

cortex are lost from the posterior and flow toward the anterior (Munro et al. 2004). In *pam-1* mutants, NMY-2 puncta often fail to clear from the posterior (Saturno et al. 2017; Figure 3C). In addition, the NMY-2 network is less robust in *pam-1* mutant embryos. Previously, we reported defects in that NMY-2 foci appeared more sparse and larger in *pam-1* embryos (Saturno et al. 2017). To quantify this, we compared images from wild-type and *pam-1* mutant embryos at two time points relative to pronuclear envelope breakdown (NEBD). In wild-type embryos at -700 seconds prior to NEBD, initial clearing of NMY-2 foci at the posterior is evident. Shortly afterward, at -500 seconds before NEBD, full posterior clearing and a pseudocleavage furrow are observed. In contrast, in *pam-1* mutants, many embryos do not show these polarity landmarks. Although wild-type embryos show posterior clearing 100% of the time, we observed partial clearing in only 61% of *pam-1* embryos ($n = 18$). We measured the number and size of the NMY-2 foci at these two time points. Although the number of foci was not significantly different, we did observe that *pam-1* embryos had smaller foci at both time points as compared with wild-type (Figure 3C and Table 5). These problems with the actomyosin cytoskeleton are likely to contribute to the polarity problems in *pam-1* mutants (Saturno et al. 2017).

To determine if *wee-1.3(lz5)* improves the actomyosin network of *pam-1* embryos, we compared the network at comparable times. *pam-1(or403)* embryos with and without *wee-1.3(lz5)* had comparable NMY-2 networks and puncta sizes. Both the number of foci and the sizes of the foci were similar in these strains (Table 5). In addition, 38.5% of embryos failed to clear NMY-2 from the posterior, a number similar to *pam-1(or403)*. Thus, the rescue of polarity landmarks by *wee-1.3(lz5)* was not due to an improvement of the actomyosin cytoskeleton dynamics.

pam-1 and *wee-1.3* interact during oocyte maturation

WEE-1.3 plays a well-established role in oocyte maturation (Burrows et al. 2006). When *wee-1.3* is inactivated, oocytes

Table 4 Size of PAR-1 domains

Genotype	Size (% embryo length) of posterior PAR-1 domain
+/+	42.03 ± 0.89 ($n = 32$)
<i>pam-1(or403)</i>	30.56 ± 1.44 ($n = 46$) ^{***}
<i>pam-1(or403); wee-1.3(lz5)</i>	42.72 ± 1.13 ($n = 47$)

PAR-1 domain size was measured for all embryos with posterior localization. Size and standard error is reported. There was a significant difference between wild-type and *pam-1(or403)* domain size, but not wild-type and *pam-1(or403); wee-1.3(lz5)* domain sizes.

^{***} $P < 0.001$

Table 5 Number and size of NMY-2 foci

Genotype	Number of NMY-2 foci		Size of NMY-2 foci (μm^2)	
	-700 seconds	-500 seconds	-700 seconds	-500 seconds
+/+	39.33 ± 5.49	29.17 ± 5.89	3.62 ± 0.22 [*]	2.93 ± 0.43 [*]
<i>pam-1(or403)</i>	29.90 ± 2.57	21.30 ± 5.52	2.61 ± 0.30	1.62 ± 0.21
<i>pam-1(or403); wee-1.3(lz5)</i>	29.75 ± 1.76	27.62 ± 4.47	2.69 ± 0.48	2.23 ± 0.53

Data gathered from confocal images at 700 and 500 seconds prior to pro-NEBD (see Materials and methods). Averages and standard error shown for wild-type ($n = 8$), *pam-1* ($n = 10$), and *pam-1; wee-1.3* ($n = 8$). T-Tests to compare each strain to *pam-1* shows no difference in the number of foci, but a difference in area between wild-type and *pam-1*.

^{*} $P < 0.05$

precociously mature. Due to the interactions of *pam-1* and *wee-1.3* in the early embryo, we asked if they also interact during oocyte maturation. First, we compared the maturation state of oocytes in wild-type and *pam-1* strains. To do this, we used DIC microscopy to score the presence of the nucleolus in the oocyte nuclei, a sign of immature oocytes. The *C. elegans* gonad is arranged with a row of maturing oocytes at the promimal end. The most proximal oocyte, closest to the spermatheca is numbered -1 with additional oocytes numbered as -2, -3 as they are arranged distally (McCarter et al. 1999). In wild-type gonads, the -1 oocyte is the most mature and usually does not have a nucleolus, whereas the -2 oocyte has a nucleolus about 40% of the time (Figure 4). A previous study suggested that *pam-1* mutants are slower to mature, with more oocytes showing a nucleolus than wild-type (Althoff et al. 2014). However, when we compared wild-type with *pam-1(or403)* or *pam-1(or347)*, we detected no significant difference in the maturation status of the oocytes (Figure 4A), suggesting that *pam-1* on its own does not affect this maturation marker.

Next, we compared the maturation state of oocytes in worms with the suppressing missense mutation *wee-1.3(syb1738)* and observed no difference in the presence of the nucleolus (Figure 4A). The maturation state of *wee-1.3(syb1738)* oocytes did not differ significantly from wild-type, in contrast to previous findings that *wee-1.3(RNAi)* oocytes precociously mature (Burrows et al. 2006); therefore, we hypothesize that the missense mutation in *wee-1.3* is not a complete loss-of-function mutation.

Similar to past work, when we inactivated *wee-1.3* by RNAi in wild-type worms, we saw a dramatic oocyte maturation effect (Burrows et al. 2006). First, we observed sterility (Figure 4B). We compared the number of embryos laid on control and *wee-1.3(RNAi)* plates between 24 and 28 hours and saw that wild-type worms treated with *wee-1.3(RNAi)* laid significantly fewer embryos. Wild-type worms on *wee-1.3(RNAi)* plates laid only 3.8% of the embryos laid on control RNAi plates (Figure 4B). When looking at the oocytes, we saw a great reduction in the number of oocytes that had a nucleolus (Figure 4, C and D). In control RNAi treatment, the nucleolus is normally present in oocytes -2 through -5; however, when *wee-1.3* was inactivated, there were significantly fewer nucleoli present (Figure 4, C and D).

To see if *wee-1.3* and *pam-1* interact in oocyte maturation, we performed the same inactivation studies in two *pam-1* backgrounds. When we inactivated *wee-1.3* in *pam-1* worms, we saw a reduction in the number of sterile worms as well as a much less pronounced oocyte maturation defect (Figure 4). After being placed on *wee-1.3(RNAi)* plates, *pam-1(or403)* worms laid 25% of the embryos laid on control RNAi plates. An even stronger interaction was observed for *pam-1(or347)* worms, which laid a comparable number of embryos on control and *wee-1.3(RNAi)* plates (Figure 4B). Additionally, the oocyte maturation defect normally induced by *wee-1.3(RNAi)* was not observed to the same degree in

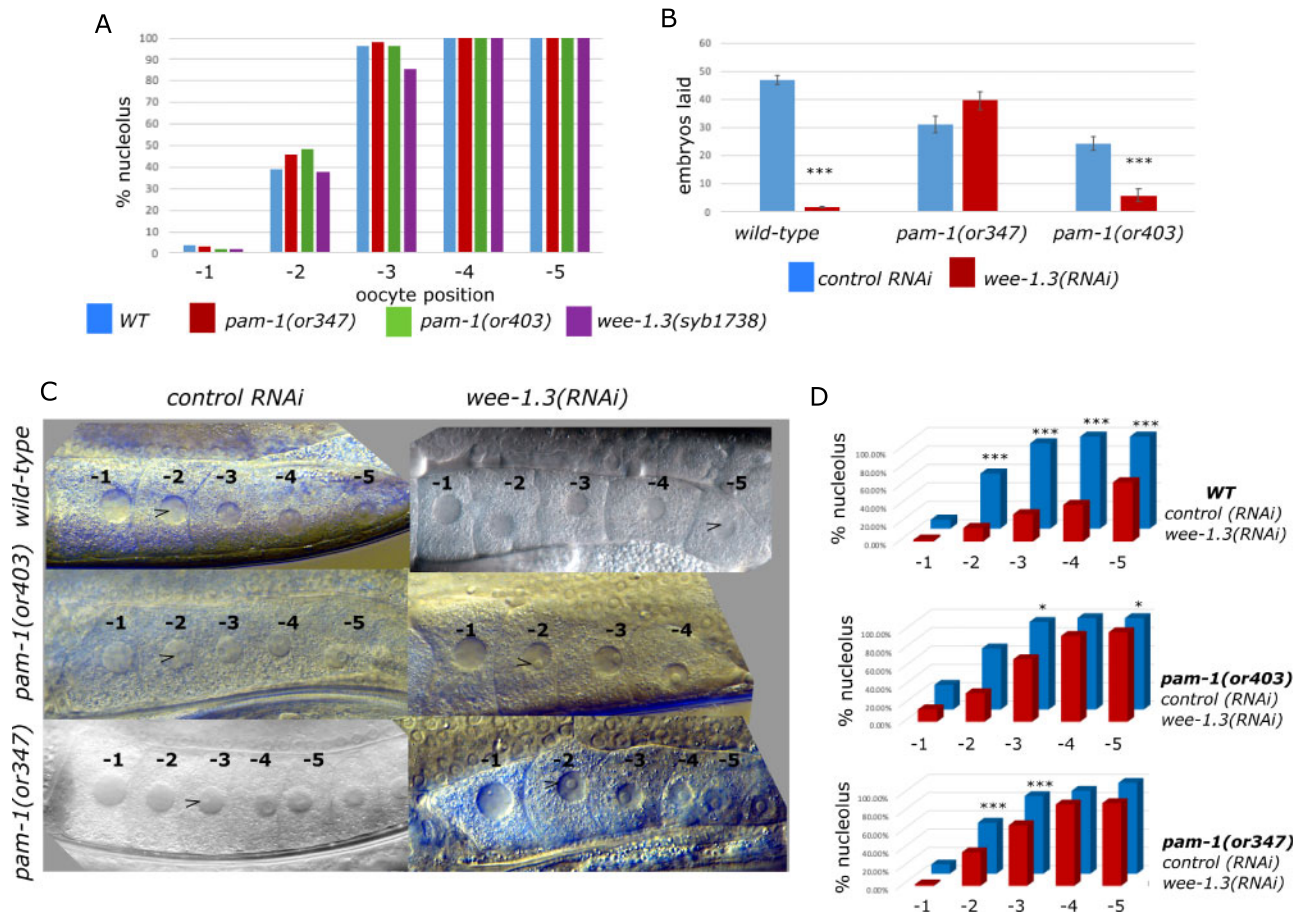


Figure 4 *pam-1* and *wee-1.3* interact during oocyte maturation. Oocytes are arranged and numbered starting from the most proximal and mature (-1) oocyte near the spermatheca. (A) Oocyte maturation is similar in *pam-1* and *wee-1.3(syb1738)* strains in comparison to wild-type as scored by the presence of the nucleolus. At least 50 gonads were scored for each strain. (B) Although wild-type worms go sterile after treatment with *wee-1.3(RNAi)*, this was reduced in *pam-1* strains as seen by continued production of embryos. Data from 20 worms per treatment. (C, D) When *wee-1.3* is inactivated by RNAi, precocious oocyte maturation is observed in wild-type worms, but not in *pam-1* worms. At least 40 gonads were scored for each treatment. (C) DIC images show one gonad arm starting with the -1 oocyte on the left. Arrowhead points to the first appearance of a nucleolus in the oocytes. (D) Quantification of nucleolus presence in the first five oocytes in RNAi of *wee-1.3* in compared with empty vector, L4440. Chi square analysis was performed for each strain between L4440 and *wee-1.3(RNAi)* * $P < 0.05$; *** $P < 0.001$

pam-1 strains. When we compared the presence of the nucleolus between *pam-1*; *wee-1.3(RNAi)* treated worms with *pam-1* control RNAi worms, we observed no differences in oocyte maturation levels in some of the oocytes (Figure 4, C and D). For instance, in *pam-1(or347)*, there was no difference in the presence of nucleoli in the -4 and -5 oocytes. In *pam-1(or403)* worms, there was no difference observed in the -2 and -4 oocytes on *wee-1.3(RNAi)* as compared with control RNAi. Thus, the precocious oocyte maturation phenotype in *wee-1.3(RNAi)* worms was lessened by mutation of *pam-1*. These data suggest that WEE-1.3 and PAM-1 interact during oocyte maturation. The presence of *pam-1* mutations partially protects the worms from sterility and defects in oocyte maturation.

WEE-1.3 localization and levels are unchanged in *pam-1* oocytes

As PAM-1 and WEE-1.3 interact during development, we wanted to test if PAM-1 regulates WEE-1.3 protein levels. To test this, we quantified WEE-1.3 fluorescence intensity in developing oocytes using a *wee-1.3::gfp* strain. This CRISPR tagged locus added GFP to the C terminus of the endogenous *wee-1.3* locus (Fernando et al. 2021). Gonads from *pam-1* and wild-type worms were compared for WEE-1.3 levels in developing oocytes. The mean intensity of

cytoplasmic WEE-1.3::GFP was comparable in wild-type and *pam-1* worms (Figure 5). We also did not note any differences in the localization of WEE-1.3 between the strains. These data suggest that PAM-1 does not regulate WEE-1.3 levels in oocytes.

To see if *wee-1.3(RNAi)* affected WEE-1.3 levels differently between WT and *pam-1* mutants, we compared WEE-1.3::GFP levels after RNAi treatment. Both *pam-1(or403)* and wild-type strains showed reduced and comparable WEE-1.3::GFP levels after treatment (Figure 5B). Thus, the difference in phenotype between the strains was not a result of differences in WEE-1.3 protein levels in treated strains.

Discussion

Here, we describe the identification of three novel suppressors of *pam-1*, which partially rescue the maternal-effect embryonic lethality and polarity defects of *pam-1* mutants. In one of these suppressors, we identified a missense mutation in *wee-1.3* and we showed that *pam-1* and *wee-1.3* interact in multiple developmental contexts.

Isolation and initial characterization of suppressors

Our genetic approach to identifying factors that may interact with *pam-1* yielded four alleles of three suppressor loci. Each

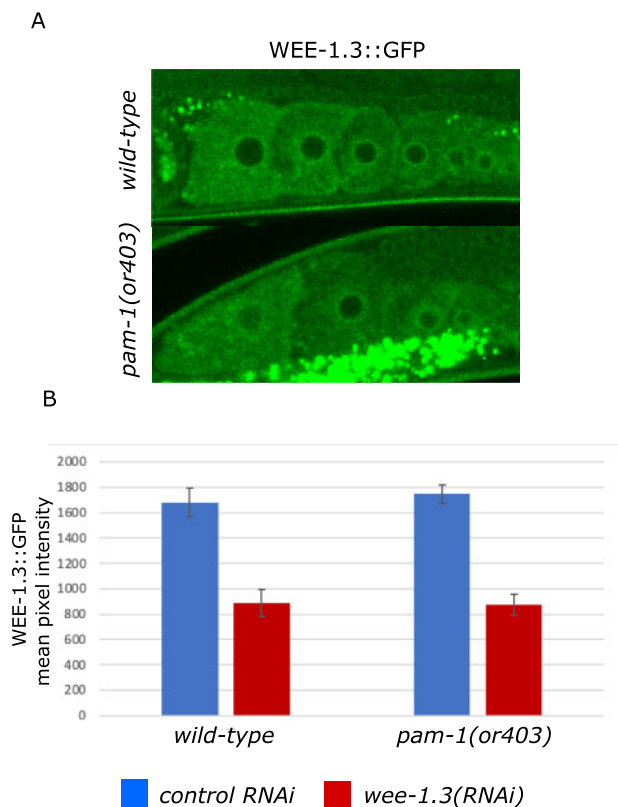


Figure 5 WEE-1.3 levels are comparable in wild-type and *pam-1* oocytes. Confocal images of WEE-1.3::GFP show no difference in the localization of WEE-1.3 in wild-type ($n = 19$) and *pam-1* mutant ($n = 16$) oocytes. The bright dots in the lower panel are autofluorescence of gut granules. (B) When the intensity of WEE-1.3 was compared in each oocyte, (-1 oocyte shown here) no difference was determined between strains; however, RNAi of *wee-1.3* (WT $n=13$ and *pam-1* $n = 9$) significantly reduced the levels. ANOVA $P < 0.001$.

suppressor mutation partially rescues the maternal-effect lethality associated with *pam-1* mutants and acts in a recessive manner. Although recessive on their own, worms heterozygous for two suppressor mutations do have some improvement in the number of embryos that hatch (Table 2). Although they do not raise hatch rates to levels found for homozygous suppression, some combinations, for instance *pam-1*(or347); *lz4*/+ *lz6*/+, suppress at levels comparable to other suppressors, like *pam-1*(or347); *wee-1.3*(*lz5*). This suggests there may be nonallelic non-complementation between the suppressors. Thus, it is possible that these suppressors act together in a pathway to suppress *pam-1* phenotypes.

Each of our new suppressors works to partially rescue the polarity defects associated with *pam-1* mutants (Figure 1). Significantly more embryos underwent pseudocleavage, a sign of cortical polarization (Hird and White 1993) and divided asymmetrically when the suppressor was present. Although we currently do not know the mechanism for this suppression, future work to identify the causative mutations will provide new insights into PAM-1's function and its role in polarization, and is likely to reveal targets of the aminopeptidase and/or factors that regulate the cytoskeleton, centrosome positioning, and cell-cycle regulation.

Identification of *wee-1.3* as a suppressor of *pam-1*

We identified a missense mutation in *wee-1.3* an inhibitory kinase, homologous to Myt1, involved in cell-cycle regulation

through inhibition of the maturation promoting factor (MPF). The MPF is made up of CDK-1 and cyclin B which drives entry into M phase of the cell cycle. Phosphorylation of CDK-1 by WEE-1.3 inhibits the complex, whereas the CDC-25 phosphatase removes the inhibitory phosphorylation to reverse the process. Activation of CDK-1 creates a feedback loop by activating CDC-25 and inhibiting WEE-1.3 to ensure quick activation of the complex (reviewed in van den Heuvel 2005). These proteins work together to ensure transient activation of MPF at the G2/M cell-cycle transition. Loss of function of *wee-1.3* in *C. elegans* results in precocious oocyte maturation, whereas gain-of-function mutations cause male sterility due to defects in spermatogenesis (Lamitina and L'Hernault 2002; Burrows et al. 2006). Since our missense mutations in *wee-1.3* did not cause any of the previously observed phenotypes on their own, we do not think the mutations in *wee-1.3* cause a complete loss of function but are instead specific to suppression of *pam-1*. The amino acid change is in a region with no known functional domains, so we do not yet understand how it affects WEE-1.3 activity. Based on the reduced viability of embryos produced by *wee-1.3*(*q89eb60*)/*wee-1.3*(*lz5*) worms, it could be that these *wee-1.3* alleles are hypomorphic.

wee-1.3(*lz5*) partially rescues polarity of *pam-1* embryos without affecting the centrosome or the cytoskeleton

The polarization problems in *pam-1* were previously tied to shortened centrosome-cortical contact times and defects in the actomyosin cytoskeleton (Saturno et al. 2017). Although we previously reported the NMY-2 foci appear larger in *pam-1* mutants, we had not measured the foci or time-matched the embryos. Here we showed that *pam-1* embryos have smaller NMY-2 foci when compared with time-matched controls, providing further evidence that PAM-1 regulates the actomyosin cytoskeleton. From phenotypic analysis, it appears that the suppressor does not act at the source of the problem. Suppressed embryos still exhibited very short centrosome-cortex contact and the cortical cytoskeleton looked similar in suppressed and non-suppressed strains. Despite this, pseudocleavage, posterior PAR-1 localization, and the asymmetric first division were largely rescued. Thus, *wee-1.3*(*lz5*) acts not to correct the problem of centrosome contact or cytoskeletal organization, but to alleviate the polarity defect by increasing the number of embryos properly localizing the PAR proteins. Whether this interaction is related to WEE-1.3's role in cell-cycle regulation or a novel function will require further study.

WEE-1.3 and PAM-1 interact in oocyte maturation

WEE-1.3 acts in oocyte maturation in *C. elegans*. Oocytes are lined up from the -1 position just adjacent to the spermatheca with this oocyte being the most mature. Mature oocytes like the -1 to -2 oocyte have condensed chromosomes and lack a nucleolus. In comparison, immature oocytes instead have a visible nucleolus (Hendzel et al. 1997; McCarter et al. 1999; Hsu et al. 2000). WEE-1.3 acts in immature oocytes to keep MPF inactive and oocytes immature (Burrows et al. 2006). When *wee-1.3* is inactivated by RNAi, oocytes precociously mature, whereas inactivation of *cdk-1* causes oocyte maturation mature. In the double inactivation, the *cdk-1* phenotype is seen, clearly showing that WEE-1.3 acts to inhibit CDK-1 in this system, similar to their interaction during mitosis (Burrows et al. 2006). When we inactivated *wee-1.3* via RNAi, we observed these same phenotypes; however, they were not present in *wee-1.3*(*syb1738*) or *wee-1.3*(*lz5*) worms (Figure 4). This suggests the missense allele does not significantly compromise WEE-1.3 function during oocyte maturation.

Previous work on PAM-1 in the *C. elegans* gonad suggests that it is one of a few peptidases in this family that regulates reproductive success (Althoff et al. 2014). Although this prior study documented a subtle delay in oocyte maturation in *pam-1* worms (Althoff et al. 2014), we did not see the same. There was no significant difference in the presence of the nucleolus in the oocytes of *pam-1* as compared with wild-type gonads (Figure 4). This difference between our data and the prior study may be due to differences they report in oocyte maturation in wild-type (Althoff et al. 2014), which varies from our work and other studies (Burrows et al. 2006). When *wee-1.3* was inactivated by RNAi, we saw a strong difference in oocyte maturation between wild-type and *pam-1* strains. This effect was clearly seen by the prevention of sterility in *pam-1* worms in which *wee-1.3* is inactivated. The oocytes in *pam-1* treated with *wee-1.3*(RNAi) did not exhibit the same precocious oocyte maturation seen when *wee-1.3* was inactivated without the *pam-1* mutation. Thus, mutations in *pam-1* partially protect worms from precocious oocyte maturation, suggesting a role for the aminopeptidase in the process.

Allele specificity

wee-1.3(lz5) is able to suppress both a missense and nonsense allele of *pam-1*. Although embryonic viability improved more in the presence of the nonsense allele, *pam-1*(or403), the extent of polarity rescue was comparable with either *pam-1* allele. Our previous work showed that in our nonsense allele, no detectable PAM-1 protein was observed after antibody staining (Fortin et al. 2010). Thus, for polarity rescue, it is unlikely that *wee-1.3*(lz5) works to restore PAM-1 function but may instead work downstream or bypass the requirement for functional PAM-1. Future work with our additional suppressors will reveal if this is a common trend or if some are allele specific suppressors.

Although rescue of embryonic viability was higher for the suppressed nonsense allele, when looking at interactions in the gonad, we saw something different. The nonsense allele of *pam-1* was not as protective as the missense allele when *wee-1.3* was inactivated by RNAi. Although both *pam-1* strains were less sensitive to precocious oocyte maturation, only the missense allele fully protected against the sterility associated with loss of *wee-1.3*. Thus, the interactions of *wee-1.3* and *pam-1* alleles vary in different contexts and may indicate differences in how WEE-1.3 and PAM-1 interact in these different developmental processes. Perhaps partial PAM-1 function is needed in the gonad for the interaction with *wee-1.3*. Similarly, it could be that the *pam-1*(or347) and *pam-1*(or403) alleles differentially regulate WEE-1.3 levels or activity to account for these differences. As we learn more about the interaction, this may become more clear.

Mechanism of action

One important function for aminopeptidases is the degradation of short peptides during the final stage of proteolysis. During certain dynamic cellular processes like cell division or gamete maturation, proteins must be removed from the cell. These proteins are tagged with ubiquitin before being degraded by the proteasome, resulting in short peptide sequences (Glotzer et al. 1991). In order to conserve resources, cells repurpose these peptides by breaking them down into individual amino acids. Protein degradation is also vital for the first cellular division. For example, in order to transition from oocyte meiosis to embryonic mitosis, the microtubule severing complex MEI-1 must be degraded (Lu and Mains 2007). Given the importance of protein degradation in these processes and significance of aminopeptidases in the

degradation pathway, it is possible that PAM-1 plays several roles in the transition from oocyte to embryo.

How then do *wee-1.3* and *pam-1* interact? One possibility for the mechanism of action is that WEE-1.3 may be a direct target of PAM-1. If this were true, we should observe higher levels of WEE-1.3 in *pam-1* mutants. However, both the levels and localization of WEE-1.3 in the gonad were unchanged in *pam-1* mutants and RNAi reduced WEE-1.3 levels comparably in both control and *pam-1* mutant strains (Figure 5). However, WEE-1.3 may be processed by PAM-1 without being totally degraded. Another possibility that we can test in the future is a change in activity. WEE-1.3 may be overactive in *pam-1* mutants, and perhaps the point mutation in the protein may alleviate the effect. *wee-1.3*(lz5) may also reduce the activity of the inhibitory kinase, allowing activation of another protein that bypasses the requirement for PAM-1. Our finding that *pam-1* worms are less sensitive to reduction of *wee-1.3* function via RNAi, and the possible hypomorphic nature of *wee-1.3*(lz5) are both consistent with these possibilities.

Another possibility is that PAM-1 regulates another component of the cell-cycle machinery. PAM-1 may positively regulate CDC-25 or MPF components. Work in *Dictyostelium* has shown that a PSA can associate with Cdk5 and regulate its localization and activity (Huber and O'Day 2011; Huber et al. 2013). This work, coupled with the role of PSAs in regulating mitosis and meiosis suggest that this interaction with WEE-1.3 and components of the MPF may be relevant for more than just *C. elegans* (Constam et al. 1995; Osada et al. 2001; Lyczak et al. 2006). A further look into the role of PAM-1 in the cell cycle may provide insights.

Still another possibility is that PAM-1 directly or indirectly affects OMA-1/-2, protein implicated in the oocyte to embryo transition. Levels of OMA-1 and the closely related OMA-2 are high in maturing oocytes but the proteins are degraded during mitosis (Detwiler et al. 2001; Shimada et al. 2002). This degradation requires the dual-specificity kinase, MBK-2, as well as CDK-1, and cyclin B3 (Shirayama et al. 2006). OMA-1 regulation spans the oocyte to embryo transition, including polarization of proteins in the one-cell embryo. Likewise, interactions we have seen between PAM-1 and WEE-1.3 work together during oocyte maturation and polarization. Future work will focus on this and other potential interactions to determine the mechanism of PAM-1 and WEE-1.3 interaction. As both PAM-1 and WEE-1.3 are conserved, it is likely that interactions we uncover may be present more broadly. By moving forward to identify the mutations in our additional suppressors we may uncover new proteins involved in cell polarity and cell-cycle regulation.

Data availability

All strains are available upon request. The authors affirm that all data necessary for confirming the conclusions of the article are present within the article, figures, and tables.

Supplementary material is available at figshare: <https://doi.org/10.25387/g3.14114156>.

Acknowledgments

Some strains were provided by the CGC, which is funded by NIH Office of Research Infrastructure Programs (P40 OD010440). Strain WDC08 was kindly provided by Anna Allen, Howard University prior to publication. The following undergraduates worked on aspects of this project over the years: Robin Alsher,

Angela Hong, Ethan Kabel, Zachary Klock, Jessica Meeker, Thuy Nguyen, Margaret Williams, and Elizabeth Wolosin.

Funding

This work was funded by NSF: IOS-0918950 to R.L., NIH: GM110614 to R.L., NIH: GM049869 and GM131749 to B.B. and J.L.

Conflicts of interest: None declared.

Literature cited

- Althoff MJ, Flick K, Trzepacz C. 2014. Collaboration within the M1 aminopeptidase family promotes reproductive success in *Caenorhabditis elegans*. *Dev Genes Evol.* 224:137–146. doi: 10.1007/s00427-014-0470-3
- Brenner S. 1974. The genetics of *Caenorhabditis elegans*. *Genetics.* 77: 71–94.
- Brooks DR, Hooper NM, Isaac RE. 2003. The *Caenorhabditis elegans* orthologue of mammalian puromycin-sensitive aminopeptidase has roles in embryogenesis and reproduction. *J. Biol. Chem.* 278: 4279–42801. doi:10.1074/jbc.M306216200
- Burrows AE, Scurman BK, Kosinski ME, Richie CT, Sadler PL, et al. 2006. The *C. elegans* Myt1 ortholog is required for the proper timing of oocyte maturation. *Development.* 133:697–709. doi: 10.1242/dev.02241
- Constam DB, Tobler AR, Rensing-Ehl A, Kemler I, Hersh LB, et al. 1995. Puromycin-sensitive aminopeptidase: sequence analysis, expression, and functional characterization. *J Biol Chem.* 270: 26931–26939. doi:10.1074/jbc.270.45.26931
- Davis MW, Hammarlund M, Harrach T, Hullett P, Olsen S, et al. 2005. Rapid single nucleotide polymorphism mapping in *C. elegans*. *BMC Genomics.* 118.6: doi:10.1186/1471-2164-6-118
- Detwiler MR, Reuben M, Li X, Rogers E, Lin R. 2001. Two zinc finger proteins, OMA-1 and OMA-2, are redundantly required for oocyte maturation in *C. elegans*. *Dev Cell.* 1:187–199. doi:10.1016/S1534-5807(01)00026-0
- Encalada SE, Martin PR, Phillips JB, Lyczak R, Hamill DR, et al. 2000. DNA replication defects delay cell division and disrupt cell polarity in early *Caenorhabditis elegans* embryos. *Dev Biol.* 228:225–238. doi:10.1006/dbio.2000.9965
- Fernando, LM, Kyrionna G, Boateng R, Allen AK, 2021. Comparison of N- and C-terminally endogenously GFP-tagged WEE- 1. 3 strains in *C. elegans*. *microPublication Biol.* doi: 10.17912/micropub.biology.000353.
- Fortin SM, Marshall SL, Jaeger EC, Greene PE, Brady LK, et al. 2010. The PAM-1 aminopeptidase regulates centrosome positioning to ensure anterior-posterior axis specification in one-cell *C. elegans* embryos. *Dev Biol.* 344:992–1000. doi:10.1016/j.ydbio.2010.06.016
- Glotzer M, Murray AW, Kirschner MW. 1991. Cyclin is degraded by the ubiquitin pathway. *Nature.* 349:132–138. doi:10.1038/349132a0
- Hendzel MJ, Wei Y, Mancini MA, Van Hooser A, Ranalli T, et al. 1997. Mitosis-specific phosphorylation of histone H3 initiates primarily within pericentromeric heterochromatin during G2 and spreads in an ordered fashion coincident with mitotic chromosome condensation. *Chromosoma.* 106:348–360. doi:10.1007/s004120050256
- Hird SN, White JG. 1993. Cortical and cytoplasmic flow polarity in early embryonic cells of *Caenorhabditis elegans*. *J Cell Biol.* 121: 1343–1355. doi:10.1083/jcb.121.6.1343
- Hodgkin J. 2005. Genetic suppression. *WormBook.* 1-13. doi: 10.1895/wormbook.1.59.1.
- Hsu J-Y, Sun Z-W, Li X, Reuben M, Tatchell K, et al. 2000. Mitotic phosphorylation of histone H3 is governed by Ipl1/aurora kinase and Glc7/PP1 phosphatase in budding yeast and nematodes: logical changes on the DNA template in an energy. *Cell.* 102:279–291.
- Huber RJ, O'Day DH. 2011. Nucleocytoplasmic transfer of cyclin dependent kinase 5 and its binding to puromycin-sensitive aminopeptidase in *Dictyostelium discoideum*. *Histochem Cell Biol.* 136: 177–189. doi:10.1007/s00418-011-0839-6
- Huber RJ, Catalano A, O'Day DH. 2013. Cyclin-dependent kinase 5 is a calmodulin-binding protein that associates with puromycin-sensitive aminopeptidase in the nucleus of *Dictyostelium*. *Biochim Biophys Acta.* 1833:11–20. doi: 10.1016/j.bbamcr.2012.10.005
- Kamath RS, Ahringer J. 2003. Genome-wide RNAi screening in *Caenorhabditis elegans*. *Methods.* 30:313–321. doi: 10.1016/S1046-2023(03)00050-1
- Kim E, Sun L, Gabel CV, Fang-Yen C. 2013. Long-Term imaging of *Caenorhabditis elegans* using nanoparticle-mediated immobilization. *PLoS One.* 8: e53419. doi:10.1371/journal.pone.0053419
- Kudo LC, Parfenova L, Ren G, Vi N, Hui M, et al. 2011. Puromycin-sensitive aminopeptidase (PSA/NPEPPS) impedes development of neuropathology in HPSA/TAUP301L double-transgenic mice. *Hum Mol Genet.* 20:1820–1833. doi:10.1093/hmg/ddr065
- Lamitina ST, L'Hernault SW. 2002. Dominant mutations in the *Caenorhabditis elegans* Myt1 ortholog wee-1.3 reveal a novel domain that controls M-phase entry during spermatogenesis. *Development.* 129:5009–5018.
- Lowry J, Yochem J, Chuang C-H, Sugioka K, Connolly AA, et al. 2015. High-throughput cloning of temperature-sensitive *Caenorhabditis elegans* mutants with adult syncytial germline membrane architecture defects. *G3 (Bethesda).* 5:2241–2255. doi: 10.1534/g3.115.021451
- Lu C, Mains PE. 2007. The *C. elegans* anaphase promoting complex and MBK-2/DYRK kinase act redundantly with CUL-3/MEL-26 ubiquitin ligase to degrade MEI-1 microtubule-severing activity after meiosis. *Dev Biol.* 302:438–447. doi:10.1016/j.ydbio.2006.09.053
- Lyczak R, Zweier L, Group T, Murrow MA, Snyder C, et al. 2006. The puromycin-sensitive aminopeptidase PAM-1 is required for meiotic exit and anteroposterior polarity in the one-cell *Caenorhabditis elegans* embryo. *Development.* 133:4281–4292. doi: 10.1242/dev.02615
- McCarter J, Bartlett B, Dang T, Schedl T. 1999. On the control of oocyte meiotic maturation and ovulation in *Caenorhabditis elegans*. *Dev Biol.* 205:111–128. doi:10.1006/dbio.1998.9109
- Minevich G, Park DS, Blankenberg D, Poole RJ, Hobert O. 2012. CloudMap: a cloud-based pipeline for analysis of mutant genome sequences. *Genetics.* 192:1249–1269. doi:10.1534/genetics.112.144204
- Munro E, Nance J, Priess JR. 2004. Cortical flows powered by asymmetrical contraction transport PAR proteins to establish and maintain anterior-posterior polarity in the early *C. elegans* embryo. *Dev Cell.* 7:413–424. doi:10.1016/j.devcel.2004.08.001
- Nance J, Zallen JA. 2011. Elaborating polarity: PAR proteins and the cytoskeleton. *Development.* 138: 799–809. doi:10.1242/dev.053538
- O'Rourke SM, Carter C, Carter L, Christensen SN, Jones MP, et al. 2011. A survey of new temperature-sensitive, embryonic-lethal mutations in *C. elegans*: 24 alleles of thirteen genes. *PLoS One.* e16644.6: doi:10.1371/journal.pone.0016644
- Osada T, Watanabe G, Kondo S, Toyoda M, Sakaki Y, et al. 2001. Male reproductive defects caused by puromycin-sensitive aminopeptidase deficiency in mice. *Mol Endocrinol.* 15:960–971. doi: 10.1210/mend.15.6.0643

- Peer WA. 2011. The role of multifunctional M1 metallopeptidases in cell cycle progression. *Ann Bot.* 107:1171–1181.
- Poloz Y, Catalano A, O'Day DH. 2012. Bestatin inhibits cell growth, cell division, and spore cell differentiation in *Dictyostelium discoideum*. *Eukaryot Cell.* 11:545–557. doi:10.1128/EC.05311-11
- Ren G, Ma Z, Hui M, Kudo LC, Hui K-S, et al. 2011. Cu, Zn-superoxide dismutase 1 (SOD1) is a novel target of Puromycin-sensitive aminopeptidase (PSA/NPEPPS): PSA/NPEPPS is a possible modifier of amyotrophic lateral sclerosis. *Mol Neurodegener.* 6: 29. doi: 10.1186/1750-1326-6-29
- Rose L, Gönczy, P. 2014. Polarity establishment, asymmetric division and segregation of fate determinants in early *C. elegans* embryos. *WormBook.* 1–43.
- Sánchez-Morán E, Jones GH, Franklin FCH, Santos JL. 2004. A puromycin-sensitive aminopeptidase is essential for meiosis in *Arabidopsis thaliana*. *Plant Cell.* 16:2895–2909. doi:10.1105/tpc.104.024992
- Saturno DM, Castanzo DT, Williams M, Parikh DA, Jaeger EC, et al. 2017. Sustained centrosome-cortical contact ensures robust polarization of the one-cell *C. elegans* embryo. *Dev Biol.* 422:135–145. doi:10.1016/j.ydbio.2016.12.025
- Sharma SK, Brock DA, Ammann RR, DeShazo T, Khosla M, et al. 2002. The Cdk5 homologue, Crp, regulates endocytosis and secretion in *Dictyostelium* and is necessary for optimum growth and differentiation. *Dev Biol.* 247:1–10. doi:10.1006/dbio.2002.0684
- Shimada M, Kawahara H, Doi H. 2002. Novel family of CCCH-type zinc-finger proteins, MOE-1, -2 and -3, participates in *C. elegans* oocyte maturation. *Genes Cells.* 7:933–947. doi:10.1046/j.1365-2443.2002.00570.x
- Shirayama M, Soto MC, Ishidate T, Kim S, Nakamura K, et al. 2006. The conserved kinases CDK-1, GSK-3, KIN-19, and MBK-2 promote OMA-1 destruction to regulate the oocyte-to-embryo transition in *C. elegans*. *Curr Biol.* 16:47–55. doi:10.1016/j.cub.2005.11.070
- van den Heuvel S. 2005. Cell-Cycle Regulation. *WormBook.*
- Yanagi K, Tanaka T, Kato K, Sadik G, Morihara T, et al. 2009. Involvement of puromycin-sensitive aminopeptidase in proteolysis of tau protein in cultured cells, and attenuated proteolysis of frontotemporal dementia and parkinsonism linked to chromosome 17 (FTDP-17) mutant tau. *Psychogeriatrics.* 9:157–166. doi:10.1111/j.1479-8301.2010.00307.x

Communicating editor: M. Zetka